◆ Human Brain Mapping 36:4592–4603 (2015) ◆

Thalamocortical Interactions Underlying Visual Fear Conditioning in Humans

Chrysa Lithari,[1]* Stephan Moratti,[2,3] and Nathan Weisz[1]

[1]*Center for Mind/Brain Sciences, CIMeC, University of Trento, Italy*
[2]*Departamento De Psicología Básica I, Universidad Complutense De Madrid, Spain*
[3]*Center for Biomedical Technology, Laboratory for Cognitive and Computational Neuroscience, Universidad Politecnica De Madrid, Spain*

Abstract: Despite a strong focus on the role of the amygdala in fear conditioning, recent works point to a more distributed network supporting fear conditioning. We aimed to elucidate interactions between subcortical and cortical regions in fear conditioning in humans. To do this, we used two fearful faces as conditioned stimuli (CS) and an electrical stimulation at the left hand, paired with one of the CS, as unconditioned stimulus (US). The luminance of the CS was rhythmically modulated leading to "entrainment" of brain oscillations at a predefined modulation frequency. Steady-state responses (SSR) were recorded by MEG. In addition to occipital regions, spectral analysis of SSR revealed increased power during fear conditioning particularly for thalamus and cerebellum contralateral to the upcoming US. Using thalamus and amygdala as seed-regions, directed functional connectivity was calculated to capture the modulation of interactions that underlie fear conditioning. Importantly, this analysis showed that the thalamus drives the fusiform area during fear conditioning, while amygdala captures the more general effect of fearful faces perception. This study confirms ideas from the animal literature, and demonstrates for the first time the central role of the thalamus in fear conditioning in humans. *Hum Brain Mapp 36:4592–4603, 2015.* © 2015 Wiley Periodicals, Inc.

Key words: fear conditioning; magnetoencephalography; visual steady state; thalamus; functional connectivity

INTRODUCTION

Fear is fundamental for living organisms to associate stimuli with, and thereby predict, potential danger, thus serving a crucial survival function. In discriminative Pavlovian fear conditioning [Rescorla, 1968] a neutral stimulus (conditioned stimulus, CS+) is associated with an intrinsically aversive stimulus (unconditioned stimulus, US), e.g. a loud noise or an electrical shock, while a second neutral stimulus remains unpaired (CS−). The amygdala is commonly considered to be the region most implicated in fear conditioning. However, BOLD modulations have also been observed in a wider set of subcortical structures such as thalamus, hippocampus and anterior cingulate cortex [Büchel and Dolan, 2000; Knight et al., 2004; Sehlmeyer

Additional Supporting Information may be found in the online version of this article.

Contract grant sponsor: European Research Council (WIN2CON) (to C.L. and N.W.); Contract grant number: ERC StG 283404.

*Correspondence to: Chrysa Lithari, Center for Mind/Brain Sciences, CIMeC via delle Regole 101, Mattarello, 38123 Trento, Italy. E-mail: chrysoula.lithari@unitn.it

Received for publication 19 February 2015; Revised 6 July 2015; Accepted 4 August 2015.

DOI: 10.1002/hbm.22940

Published online 19 August 2015 in Wiley Online Library (wileyonlinelibrary.com).

et al., 2009]. Crucially, the thalamic nuclei play a major role in mediating auditory fear conditioning in rats [Apergis-Schoute et al., 2005; Quirk et al., 1997]. In a recent study, Weinberger [2011] points out that the thalamic medial geniculate nucleus is equally important for auditory fear conditioning as the amygdala. Considering the position in the hierarchy of sensory processing, he concludes that the thalamus should be considered the crucial structure in (auditory) fear conditioning. The "equipotentiality" [see Romanski and LeDoux, 1992] of thalamo-amygdala and thalamo-cortico-amygdala pathways in fear conditioning [Ledoux, 2003; Medina et al., 2002] have been confirmed in animal models [Romanski and Ledoux, 1992; Shi and Davis, 2001] and by means of functional connectivity in humans [Das et al., 2005]. However, the connectivity pattern among deep and cortical structures in fear conditioning is still an open issue.

The main goal of the present study was to investigate whether MEG could elucidate the dynamic interplay between subcortical and cortical structures [Roux et al., 2013; Tesche and Karhu, 2000a] that support fear conditioning in humans. Similar to previous works [Miskovic and Keil, 2012; Moratti and Keil, 2005, 2009; Moratti et al., 2006], we rhythmically modulated the luminance of visual CS+ and CS− stimuli. This stimulation leads to brain signals with excellent signal-to-noise ratios that are "entrained" to the a priori defined modulation frequency, the so-called steady-state responses (SSR) [Victor and Mast, 1991]. In the present study, an electrical shock on the left median nerve served as the US. We spectrally analyzed the SSR and applied beamforming techniques to project on the source level. We hypothesized that fear conditioning would not only lead to increased SSRs in the visual cortex [Moratti et al., 2006; Moratti and Keil, 2009], but also on a wider set of subcortical regions "entrained" via the flickering stimuli. Finally, we investigated functional connectivity to and from (data- and literature-driven) fear-related regions. We expected that coupling within such a network would be particularly pronounced during the CS+. To our knowledge, this is the first study that demonstrates the network dynamics between the thalamus and visual cortex during visual fear conditioning in humans.

MATERIALS AND METHODS

Participants

Twenty right-handed participants (10 females; age: 28.05 ± 3.3 years) with normal or corrected-to-normal vision, no neurological or psychiatric disorders and no family history of photic epilepsy took part in the experiment. The Ethical Committee of the University of Trento approved the experimental protocol and the experiments were undertaken with the understanding and written consent of each participant.

Stimuli and Procedure

Two fearful faces of Caucasian adult women from the Radboud Faces Database [Langner et al., 2010] were used as CS+ and CS− counterbalanced among participants. The CS was flickering at 15 Hz for 5 sec on a black screen with a refresh rate of 60 Hz (Fig. 1, top; two frames "on" and two frames "off"). Since a black screen was introduced between the face stimuli, the overall frequency of visual stimulation was at 30 Hz. The stimuli were projected on a screen inside an MEG shielded room through a video projector (Panasonic PT-D7700E) and a mirror system. The intertrial interval was jittered between 7 and 8 sec and a white cross was presented at the center of the screen. The precise start and end of each trial were determined by a photodiode sensitive to luminance change placed on the screen inside the MEG room.

The US was a 100 ms electric pulse stimulating the participant on the left median nerve. Two electrodes (cathode proximal) were connected directly to a galvanically insulated electrical stimulator. A step-wise procedure was followed before the experiment to define the individual pain threshold. Participants were asked to rate the intensity of the pulse using a scale of 0 (not perceived) to 7 (very painful). It was explained to them that the intensity used during the experiment should be tolerable, however it should be sufficiently unpleasant in order to be salient. The target rated pain level for each individual was 6 and this procedure led to an average of 33.05 ± 16.3 mA at 200 V. The delivery of the US jittered between 4,600 and 4,800 ms after the CS+ start and they terminated simultaneously.

The experiment consisted of three phases: habituation, conditioning and extinction. During habituation, 18 CS+ and 18 CS− trials were presented in random order in two blocks each lasting 6 min, but the CS+ was never paired with an US. During the conditioning phase, 40 CS+ and 40 CS− trials were presented, while CS+ trials were paired with US using a 100% reinforcement schedule that is known to lead to faster extinction [Skinner, 1953]. Conditioning included five blocks while the extinction phase was identical to the habituation. The whole experiment lasted for approximately 1 h. Participants were instructed to pay attention, as they would be asked to report the stimulus predicting the delivery of the painful stimulus at the end of each block [Knight et al., 2004; Miskovic and Keil 2013]. All participants reported that they were aware of the CS−US contingency already after the first block of conditioning.

Startle Responses

As a measure of the effect of conditioning on the activation of the defense system [Lang et al., 1990], we recorded participants' startle responses elicited by a short (100 ms) white noise presented binaurally in selected trials through a pneumatic tube system. Startle responses were extracted from the vertical Electro-occulo-graphic (EOG) bipolar recordings. For each of the three phases of the experiment 33 startle responses were recorded; 11 in CS+, 11 in CS−,

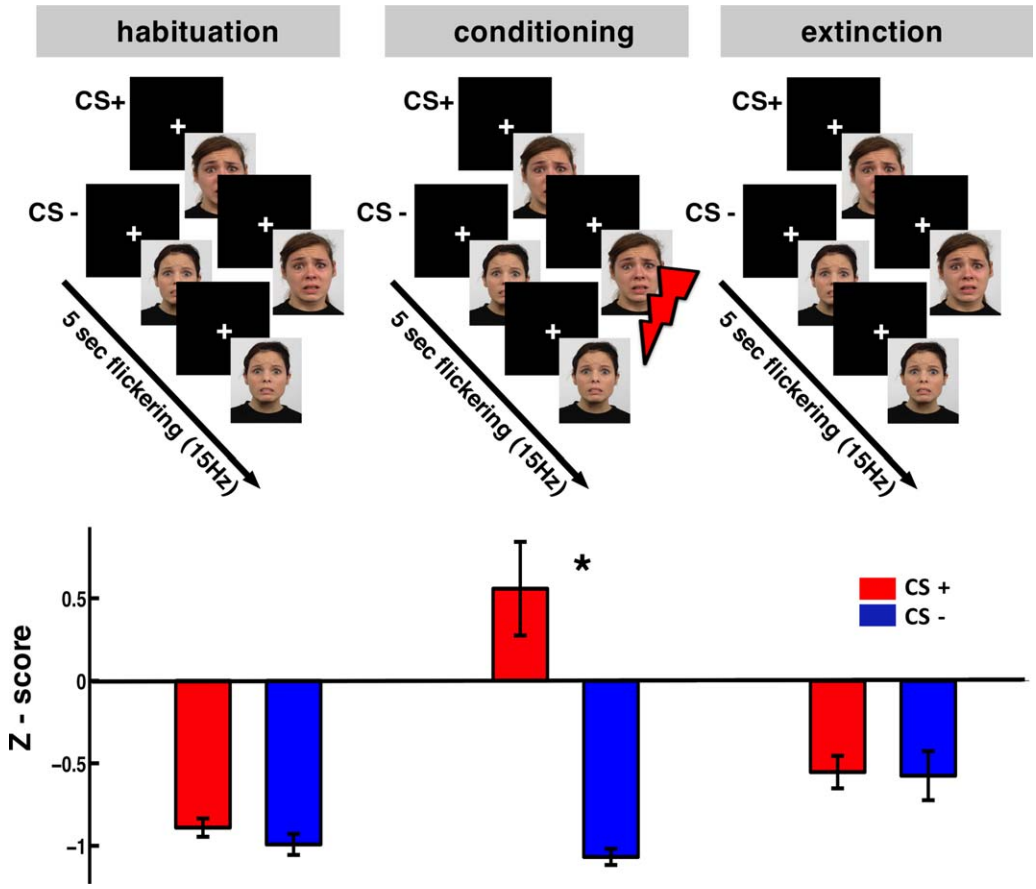

Figure 1.

Top: the experimental design. Bottom: magnitude of the eye blink startle reflex expressed as z-scores. Error bars represent the standard error across subjects. Startle reflex was modulated by the CS+ only during the conditioning phase (* $P = 0.01$). Note that the z-scores are mostly negative because participants were more "responsive" to the white noise presented during ITI than during flickering CSs.

and 11 during ITIs. Startle trials were randomly distributed in each block but a block never started with such a trial. The number of trials was equalized for CS+ and CS− after rejecting the artifact-contaminated ones. The EOG data from two participants were excluded because of recording problems. The magnitude of the startle response was calculated by subtracting the peak amplitude during 20 to 120 ms poststimulus from a 200 ms prestimulus period. The absolute values were then expressed in *z*-scores to account for individual variability [Keil et al., 2007; Stolarova et al., 2006]. Repeated-measures ANOVA was conducted with phases (habituation, conditioning, extinction) and condition (CS+, CS−, ITI) as within subject factors.

MEG Recording and Preprocessing

MEG was recorded at a sampling rate of 1 kHz using a 306-channel (204 first order planar gradiometers, 102 magnetometers) VectorView MEG system (Elekta-Neuromag Ltd., Helsinki, Finland) in a magnetically shielded room (AK3B, Vakuum Schmelze, Hanau, Germany). Head positions of the individuals relative to the MEG sensors were continuously controlled within a block using three coils placed at three fiducial points (nasion, left and right preauricular points). Head movements did not exceed 1.5 cm within and between blocks.

Data were treated offline using the Fieldtrip toolbox [Oostenveld et al., 2011]. CS+ and CS− trials of 2 sec pre- and 6 sec poststimulus were extracted from the continuous data stream based on the photodiode signal. Trials containing physiological or acquisition artifacts were visually inspected and rejected. The number of CS+ and CS− trials were equalized for each subject within each of the experimental phases to ensure that our results were not confounded by systematic differences in signal-to-noise ratio.

Analysis of Evoked Power

SSRs were first analyzed on a sensor level. On the averaged time series, i.e. the evoked response, spectral analysis was performed (Hanning tapering; 2–40 Hz in 1 Hz steps; time windows of seven cycles per frequency; sliding in 50 ms steps). Horizontal and vertical planar gradients of the magnetic field at each gradiometer were analyzed separately. The sum of both directions (combined planar gradient) was computed to obtain the power at each sensor irrespective of the orientation of the gradients [Medendorp et al., 2007]. We first verified the presence of the visual SSR caused by the flickering stimulus, irrespective of the stimuli and the experimental phase. We observed evoked oscillatory responses at 15 and 30 Hz on the sensor level and also estimated the generators of these global effects on source level (see description below). In the next step we validated evoked power differences between CS+ and CS− conditions in all experimental phases (0–4.5 sec, 2–40 Hz).

To estimate the generators of the sensor level effects, source analysis was performed using the time-domain Linearly Constrained Minimum Variance (LCMV) beamformer [Van Veen et al., 1997]. A structural MRI (4 T Bruker MedSpec, Siemens) was available for 15 out of 20 participants. Three anatomical landmarks (nasion and left/right pre auricular points) and the head shape were digitized with a Fastrak 3D digitizer (Polhemus, Colchester, VT) and co-registered on the individual segmented MRIs. Co-registered MRIs were segmented using SPM5 to derive the outer brain surface allowing the calculation of a semi-realistic head model [Nolte, 2003]. For those participants with no structural MRI, an MNI template brain was warped (affine transformation) to minimize the difference to the individually digitized head shape. An equally spaced grid (1 cm resolution) was fitted to a brain volume obtained from a segmented template MNI brain. This template grid was subsequently warped into the individual headspace ensuring the same amount of grid points at the same brain location in MNI space across participants [Larson-Prior et al., 2013]. The grid positions in individual head coordinates, the sensor positions relative to the head and the head model were used to calculate the leadfield. Both magnetometers and gradiometers were included in the source estimation after appropriate adjustment of the balancing matrix based on the distance of the gradiometers (17 mm).

To validate the quality of our recordings and the source analysis approach in general, we computed the differences between visual-steady-state stimulation (1.3–2.3 sec) and a prestimulus period (−1.2 to −0.2 sec) merging CS+ and CS− across all experimental phases. Common spatial filters were calculated using the averaged covariance matrices of prestimulus and poststimulus intervals. We bandpass filtered around the frequency of interest (13–17 Hz and 28–32 Hz) and applied spatial filters derived by the LCMV beamformer to the complex Fourier transformed averaged MEG data. The complex modulus was then determined, in order to derive the evoked magnitude of this frequency at each grid point inside the brain volume [for an analogous approach see Weisz et al., 2012; for application of LCMV beamformer filters to Fourier coefficients see, Bardouille and Ross, 2008]. The same method was followed for CS+ versus CS− comparison for poststimulus periods (0–4.5 sec). Given the sensor level spectral results, the condition contrast focused on 30 Hz for which the most pronounced conditioning effects were observed.

Functional Connectivity

Given our findings in thalamus, as well as the central role of the amygdala in fear conditioning, we intended to explore the nature of the directed connections to and from these regions. We used Phase Slope Index (PSI) [Nolte et al., 2008] as a connectivity metric implemented in FieldTrip toolbox. Coordinates for the thalamus (MNI coordinates [9, −15, 8]) were obtained in a data-driven manner, while coordinates for the amygdala seed (MNI coordinates [22, −6, −12]) were taken from a recent relevant study [see Introduction; Das et al., 2005]. A fast Fourier transform (Hanning taper) was applied on single trials (0.2–4.5 sec) and the Fourier coefficients were subsequently projected to source space using spatial filters derived from DICS. PSI was calculated for all possible pairs between the seed-voxels and all other voxels for 15 and 30 Hz. The bandwidth when calculating PSI was set to 5 Hz [Nolte and Müller, 2010]. PSI values are either positive, indicating flow of information from the seed towards another voxel, or negative, indicating afferent connections to the seed.

Statistics

On a sensor level, a dependent samples *t*-test was carried out on time-frequency data to test for differences between poststimulus versus prestimulus and between CS+ versus CS− during habituation, conditioning and extinction periods. To control for multiple comparisons, a nonparametric randomization test was undertaken [Maris and Oostenveld, 2007]. The *t*-test was repeated 1,000 times on data shuffled across conditions and the largest *t*-value of a cluster coherent in time and space was kept in memory. The observed clusters were compared against the distribution obtained from the randomization procedure and were considered significant when their probability was below 5%. The statistical analysis of the time-frequency sensor data (CS+ vs. CS−) revealed significant effects at 30 Hz, and further analysis was focused on that frequency.

To derive probable locations underlying the sensor based effects, analogous *t*-test contrasts were undertaken for the source solutions. We used a cluster-based approach commonly used in fMRI studies implemented as 3D ClustSim within the AFNI suite [Cox, 1996; Cox and Hyde, 1997], to capture the most relevant clusters. The program simulates t-values on a grid provided by the user,

thresholds them according to a P value and records the size of the remaining clusters. Ten thousand repetitions of this process give a distribution of cluster sizes describing purely random activity that can be used to assess the probability of the empirically observed clusters. We used a smoothing factor of 1cm, indicative of the MEG spatial resolution [Hillebrand and Barnes, 2002] on the random data prior to cluster identification. This led to a minimum cluster size of 17 voxels for an alpha threshold of $P \leq 0.05$. To visualize source results, the statistical values were interpolated onto a standard brain in MNI space and plotted using MRIcroGL (http://www.mccauslandcenter.sc.edu/mricrogl/).

Regarding PSI data, the same statistical approach described above was performed. PSI values can be positive or negative, so CS+ and CS− conditions were first contrasted against zero and then a CS+ vs. CS− contrast was performed.

RESULTS

Behavioral Validation of Conditioning

The startle responses of CS+ and CS− trials did not differ significantly during the habituation and extinction phases (Fig. 1, bottom). A reliable modulation was found in the conditioning phase where participants showed a higher startle response during CS+ compared with CS− ($P = 0.01$, $t = 2.89$, $df = 17$). The startle responses during the ITIs were significantly higher than both CS+ and CS− during habituation and extinction ($P < 0.001$; leading to the overall negative values), whereas during the conditioning phase they were at the same level with CS+ (data not shown). The CS+ startle responses during conditioning were significantly higher than during habituation ($P = 0.02$) while the contrast between conditioning and extinction showed only a trend ($P = 0.07$) indicating the learnt association. The startle responses during CS− and during ITIs did not show any modulation due to the experimental phase. The differentiated startle response at CS+ validates the effectiveness of classical fear conditioning as it indicates a conditioning-specific activation of the defense system [Lang et al., 1990].

Steady State Responses (SSR)

Figure 2 depicts the details of the recorded SSR used to determine if our experimental stimulus elicited robust visual SSRs independent of the condition and the experimental phase. The SSR is evident on sensor level (Fig. 2A), and on the peaks (15 and 30 Hz) at the whole-head power spectrum (Fig. 2B). The SSR is localized on posterior sensors (Fig. 2C). The time-frequency representations of evoked power changes (compared with baseline in t-values) shows sustained evoked brain activity at 15 and 30 Hz that is clearly time-locked to the stimulus onset and offset (Fig. 2D). Source analysis of this effect (Fig. 2E)

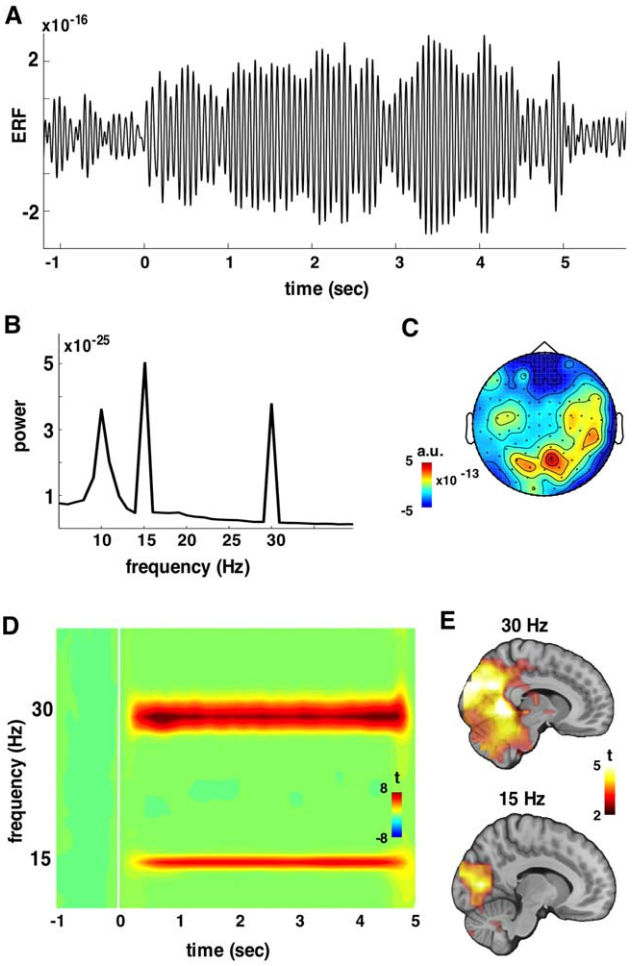

Figure 2.

SSR merged across experimental phases (habituation, conditioning, extinction) and stimuli (CS+ and CS−). The grand average SSR (filtered 2–25 Hz) from a posterior magnetometer is plotted in panel **A** including pre and poststimulus periods. In panel **B**, the whole-head power spectrum clearly shows peaks at the stimulation frequency (15 Hz) and its harmonic (30 Hz). The topography of the SSR on sensor level (magnetometers) is illustrated in **C**, where activation is maximized at posterior sensors. In panel **D**, whole-head time-frequency representation of SSR on gradiometers is depicted. SSRs are observable at 15 Hz and 30 Hz. By contrasting pre vs. poststimulus period the SSR was mainly localized on occipital gyri (BA 18 and 19) as shown in panel **E**, being overall stronger and more widespread for 30 Hz.

yielded a significant positive cluster in visual cortical areas (BA 17, 18, 19) for both 15 (size = 136 grid points) and 30 Hz (size = 516 grid points).

Enhanced SSR During CS+

A nonparametric permutation test on the time-frequency representation of the evoked SSR during conditioning

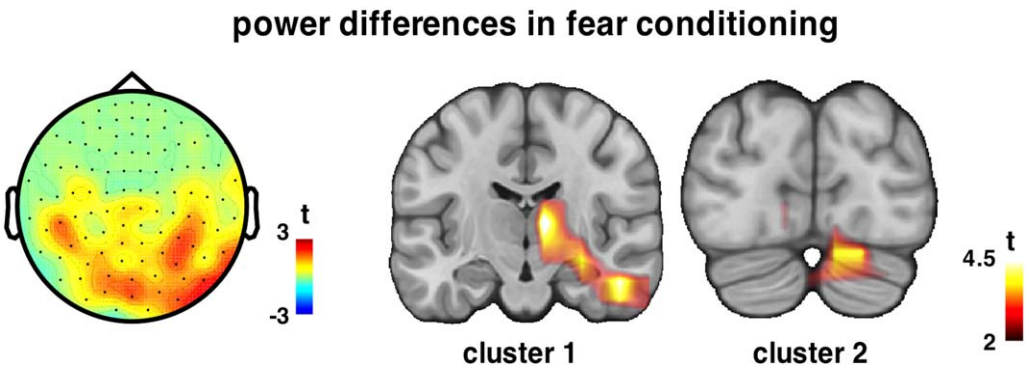

Figure 3.

Time-frequency statistics (CS+ vs. CS−) on evoked SSR resulted in one positive cluster at 30 Hz during conditioning localized on posterior sensors (gradiometers) partially lateralized to the right. Two spatial clusters on source level showed higher evoked power during the CS+ projection as compared with CS− at 30 Hz. The first cluster, lateralized contralateral to the US delivery, has its maximum in the thalamus. The second cluster comprises cerebellum, and has its maximum also at the right.

phase revealed a positive (CS+ > CS−) cluster on the gradiometers ($P < 0.001$) (Fig. 3), as well as on the magnetometers ($P = 0.02$) (data not shown) at 30 Hz. The topographies of the clusters cover posterior sensors lateralized contralateral to the upcoming US, with the effect being weaker overall on the magnetometers. Source level analysis over the whole period (0–4.5 sec) on the power of the evoked SSR revealed two positive significant clusters (Fig. 3). The strongest cluster (Cluster 1: size = 91 grid points) includes deeper structures contralateral to the electrical stimulation (US) encompassing regions such as thalamus and parahippocampal gyrus. It extends bilaterally to secondary visual cortices (BA 18, 19). The second strongest cluster (Cluster 2: size = 40 grid points) involves cerebellar structures partially lateralized to the right. No significant cluster was observed during habituation and extinction periods. To test the validity of increased SSR in depth, we performed the same analysis keeping only the 15 subjects for whom we obtained individual structural MRs, and the localization of the effect is indeed very similar (data not shown, but provided as Supporting Information): the first cluster (size = 21 voxels), lateralized contralateral to the US delivery, has its maximum in the thalamus. The second cluster (size = 15 voxels) comprises cerebellum, has its maximum also at the right, however it does not result significant with 15 participants.

Seeded Connectivity

As a final step, directed connectivity (PSI) was employed to assess the flow of information on source level to and from two seed regions. First, the thalamus (MNI [9, −15, 8]) was chosen as seed as this was where the most prominent power effect was found. Thalamic efferent connectivity was only observed during the conditioning phase. Thalamus drives precentral and postcentral gyri (BA 40, 13), insula, posterior cingulate, parahippocampal gyrus during CS+ (size = 210 grid points), while it drives caudate, middle and superior frontal gyri (BA 6, 32) during CS− (size = 76 grid points) (Fig. 4, first row). Contrasting CS+ and CS−, the increase of thalamus efferent connectivity was higher for CS+ than CS− resulting in a positive cluster (size = 54 grid points) that included deeper regions, like fusiform (BA 35, 36, 37) and parahippocampal gyri (BA 27) (Supporting Information Fig. S1). That is, thalamus connections towards fusiform were modulated by fear conditioning.

Based on its putative role in fear conditioning, a seed was placed in right amygdala [MNI [22, −6, −12]; coordinates obtained from Das et al., 2005] to examine functional connectivity from and to this region. A set of regions was found to drive neural responses in amygdala across experimental phases for both CS+ and CS− (habituation CS+: size = 62, habituation CS−: size = 24, conditioning CS+: 45, conditioning CS−: 136, extinction CS+: size = 73, extinction CS−: size = 84). The negative clusters indicated increased the flow of information towards amygdala from fusiform (BA 35, 36, 37) and parahippocampal gyri (BA 27), as well as from occipital cortex (BA 18, 19) (clusters during conditioning phase shown in Fig. 4, second row). However, this difference was not affected by conditioning and it is most probably attributed to the nature of the stimuli: both CS+ and CS− were fearful faces (see Discussion). When the seed was placed in the left amygdala, a region responsive to fearful faces (MNI [−26 0 −20]) [Vuilleumier et al., 2001], the very same effect was found also across experimental phases (data not shown).

Given the flow of information resulting from this analysis, we illustrate the observed connectivity pattern during fear-conditioning to highlight for the first time the critical role of thalamus in humans (Fig. 4, low part; see Discussion).

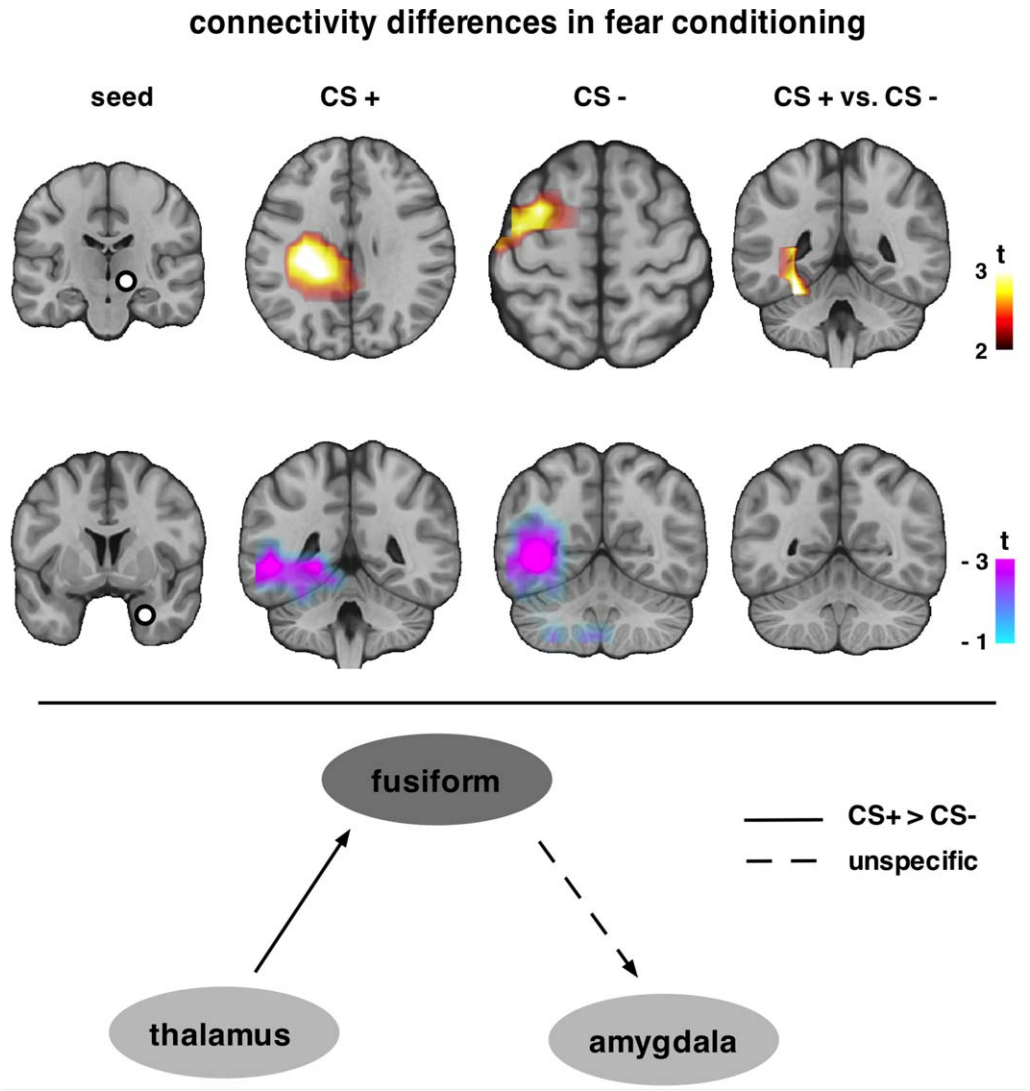

Figure 4.

A higher flow of information from a set of regions towards the thalamus was observed for both CS+ and CS− only during conditioning (first row). The cluster for CS+ included cortical and subcortical regions, while for CS− the cluster was mainly on the cortex. Fear conditioning differentiated efferent thalamic connections to fusiform, and also to subcortical regions such as parahippocampal gyrus, caudate, caudate tail and pulvinar. Amygdala afferent connectivity from the same region was increased during all experimental phases (conditioning is depicted herein), irrespective of CS+/ CS−. Data were merged across stimulus type and only the cluster during conditioning is depicted. In the lower part, the connectivity pattern suggested by our findings is illustrated. Fear conditioning modulates connectivity from thalamus to fusiform. Nonfear-specific connections were found from fusiform to amygdala.

DISCUSSION

This work aimed to elucidate the temporal dynamics of interaction between cortical and subcortical structures relevant for fear conditioning in humans. SSRs revealed increased evoked power not only in the visual cortex, but also in thalamic regions and the cerebellum contralateral to the upcoming US. To characterize the interaction patterns within a fear conditioning network, we examined functional connectivity to and from two key regions: the thalamus, where our effects were strongest; and the amygdala, considered as the brain region most implicated in fear conditioning [Maren, 2001]. To our knowledge, we demonstrated, for the first time, that the thalamus and parietal areas drive activity in extrastriate cortices during fear conditioning. Additionally, amygdala

afferent connections failed to differentiate between CS+ and CS−.

Evoked Power

Time-frequency analysis revealed increased power at 30 Hz at posterior sensors during the entire stimulation period. This effect was localized to the visual cortex in line with previous studies using a similar paradigm [Keil et al., 2007; Moratti et al., 2006; Stolarova et al., 2006]. These findings suggest facilitated sensory processing for the CS+ [Keil et al., 2007]. However, the difference in power was maximized at the thalamus contralateral to the upcoming US. The thalamus has been considered the gatekeeper for sensory input to the cerebral cortex, preventing or enhancing the passage of information flow depending on the behavioral state of the animal [Guillery and Sherman, 2002]. In humans (subcortical) paths from thalamic structures to amygdala mediate processing of affective stimuli [Pessoa and Adoplhs, 2010; Romanski and LeDoux, 1992]. Activity in human amygdala during conditioning correlates with thalamic activity but not with cortical activity [Morris et al., 1999]. Lesions in the auditory thalamus in rats disrupted fear-potentiated startle to auditory CS [Campeau and Davis, 1995], which underlies the specific involvement of thalamus in fear conditioning. The cluster we observed extends to adjacent structures like the hippocampus and cingulate. However, the amygdala, a core structure in fear conditioning [LeDoux, 2003], did not show increased SSR power. This may be explained, at least partially, by its putative learning-related role [LaBar et al., 1998; Phelps and Anderson, 1997] rather than a principal role in the online processing of fear, that might have prevented overall power effects.

Furthermore, a strong effect for increased SSR was found in the right medial cerebellum. Given the role of cerebellum in the timing of movement and sensation, particularly in the sub-second range [Rao et al., 2001; Spencer et al., 2003], one expects its prominent response to the rhythmic modulation of CS, as shown in the pre versus poststimulus analysis (Fig. 2). It is unlikely that the cerebellar response is a leakage effect from the visual cortex generated by the source localization algorithm. First, contrasting source activity maps with a control condition (here CS−) controls for such leakage effects [Cornwell et al., 2008]. Second, such a SSR response in the cerebellum has been reported using auditory SSR [Pastor et al., 2002]. Fear conditioning also differentiated this modulation. While cerebellar findings are not new in the context of fear conditioning per se [Sacchetti et al., 2002], previous reports in human have not focused on this. The role of the cerebellum in fear learning has been investigated mostly in animals and it is well known that the cerebellum is a region of motor learning, it is crucial for expressing the learnt conditioned response (i.e. eyelid reflex) [Garcia et al., 1999; Hansel et al., 2001; Sacchetti et al., 2002]. In humans, medial cerebellum, is involved in fear-conditioned potentiation of the acoustic blink reflex [Maschke et al., 2000]. The cerebellar modulation of SSR by fear relevance in our study may reflect increased sensitivity of certain motor reflexes such as the increased startle responses.

One could argue that the increased SSR in thalamus reflects the expectation of the US and rather than fear conditioning. Indeed it is known for all sensory modalities that expectancy activates a vast set of cortical and subcortical regions [Langner et al., 2011]. Furthermore, it is likely that expectancy, at least partially, could play a role in fear conditioning [Vuilleumier and Driver, 2007]. However, for two reasons it is unlikely that our thalamic finding could be attributed to expectancy alone: Firstly our analysis emphasizes phase alignment with the modulation rate of the CS, whereas the expectation of the US is at a different (slower) temporal scale. If expectancy plays a role, it is thus likely to be more pronounced at slower frequencies, for which we found no evidence. Secondly and more interestingly, neural activity on both modality specific (visual) and modality unspecific (supplementary motor) areas is linearly associated to the strength of CS-US pairing and is decreased as a function of expectancy [Moratti and Keil, 2009]. However and in line with previous literature [Keil et al., 2007], we report *increased* SSR for CS+ in cortical areas specific to the CS modality.

Overall, we observed a set of cortical and subcortical regions exhibiting higher power at the stimulation frequency for the CS+, confirming our hypothesis. Capturing neuronal dynamics in deeper brain structures such as the thalamus or amygdala using MEG or EEG can be seen as a challenge in itself, even though an increasing amount of works do indicate its feasibility [Balderston et al., 2013; Bish et al., 2004; Brookes et al., 2011; Cornwell et al., 2008; Jerbi et al., 2007; Lou et al., 2010; Martin et al., 2005; Poch et al., 2011; Roux et al., 2013; Tesche and Karhu, 2000b; Timmermann et al., 2002]. Specifically, Quaraan et al. [2010] show that recording activity from hippocampus is possible when (a) there is high signal-to-noise ratio, which is undebated with SSR and (b) a control condition is used to confront eventual leakage from the visual cortex in deep sources, that is, in our case the CS−. We consider the fact that the "blurry" resolution when clustering over large spatial extent favors the statistical strength. However, the separate maxima (CS+ vs. CS− on thalamus, pre vs. poststimulus on visual cortex) speak against the idea of a cortical activation that smears into thalamus. Furthermore, our MEG analysis includes magnetometer sensors, which are sensitive to deeper sources [Tarkiainen et al., 2003]. Finally, due to the consistent finding of thalamus and cerebellum activity in fear conditioning in the literature and the high signal-to-noise ratio using SSRs, we are confident about the localization of deep structures.

Functional Connectivity in Fear Conditioning

The main objective of our study was to characterize functional subcortical-cortical connections during fear

conditioning. The seed in the thalamus was selected in a data-driven way, since the power analysis primarily highlighted its role in fear conditioning. Efferent thalamic connections towards posterior fusiform and parahippocampal gyri differentiated between CS+ and CS−. To our knowledge, this is the first MEG study to highlight the critical role of the thalamus in fear conditioning in humans, supporting recent animal studies [Apergis-Schoute et al., 2005; Weinberger, 2011]. Using face stimuli as CSs, such a modulation of thalamo-fusiform connectivity is likely given the dense anatomical projections of the fusiform gyrus to the thalamus [Clarke et al., 1999]. The possibility that the thalamo-fusiform connectivity is present whenever a sensory event is expected cannot be excluded, but it is highly improbable, given the thalamo-fusiform projections and the well defined role of fusiform in high-level visual processing, especially facial stimuli [McCarthy et al., 1997].

Although there were no evoked power effects in the amygdala, placing a seed [Sun et al., 2004] in this region yielded meaningful results. However, the amygdala failed to capture fear-conditioning effects. Instead, capturing the more general effect of fearful faces used as CS during the whole experiment, indicative of emotional processing. Whether using a meaningless CS (e.g. a Gabor grating), rather than fearful faces, would show amygdala modulation remains to be examined. A previous fMRI study investigated effective connectivity and mentioned the amygdala as a key source of afferent and efferent connections during conditioning [Alvarez et al., 2008]. Here we identified thalamus as the core subcortical structure mediating fear conditioning. The main differences between the study of Alvarez and ours are: First, our findings were observed in the context of SSRs, where the recorded brain activity is paced by the stimulus in a strict temporal manner. Second, we used fearful faces instead of a contextual paradigm (virtual environment) which is considered to be converged with US in the amygdala [Maren, 2001].

One could raise some concern on the simplified directional model we propose. We are aware that (a) there are definitely more structures involved in the brain functional network during fear conditioning probably observable with all-to-all connectivity analysis and (b) this is not the mechanism that the brain uses to prompt SSR modulations in fear conditioning. Our intension is to just describe our findings in a schematic way and highlight the role of thalamus.

According to the "low road" hypothesis, a specific subcortical route (colliculus-pulvinar-amygdala) of information processing, the so-called 'low road' facilitates emotional processing. However, studies in humans do not support such a separate circuit for emotional processing bypassing the cortex [Piech et al., 2010; Tsuchiya et al., 2009; Vuilleumier, 2005]. Instead, pulvinar, a thalamic structure absent in rodents, seems to function more as a "control site," densely connected to the visual cortex [Shipp, 2003, 2004] that coordinates and regulates flow of information on the cortex. So, according to the multiple-waves hypothesis [Pessoa and Adolphs, 2010] the cortex has a more important role in emotion processing than it was traditionally assumed. Taken together the power effect (thalamus and extrastriate cortex) and the connectivity effect (thalamus towards extrastriate cortex), our findings can be considered under the "multiple-waves" hypothesis.

In conclusion, exploring entrainment by means of steady-state stimulation, we observed subcortical-cortical network dynamics during fear conditioning that reflect an increased gating of modality-specific sensory information. Crucially, our approach elucidated the central role of thalamus in fear conditioning in humans that has only been described in animal models so far.

Limitations and Experimental Paradigm Issues

It is known that thalamus is a complex structure with multiple substructures involved in different cognitive processes and anatomically is divided in nuclei that project to auditory, visual and sensory cortices [White, 1979]. However, the spatial resolution of MEG is not fine enough to discriminate the involvement of different thalamic nuclei in fear conditioning. The same stands for amygdala, for which—with the spatial resolution of the MEG—we find responses to the fearful faces in general, rather than responses specific to fear learning. Thus potential involvement of lateral amygdala in fear conditioning [LeDoux et al., 1990] cannot be excluded. However, the use of steady state stimulation allows looking for differences on those regions, which are responsive to the entrainment. This, on one side seems to limit our research as compared with event-related potentials, which describe brain activity free of any frequency modulation from the part of the experimenter. On the other side, SSR offer an extremely high signal-to-noise ratio that is a prerequisite to reveal differences in deeper regions (e.g. hippocampus) with MEG [Quaraan et al., 2010].

Herein we dealt with visually elicited fear conditioning. Whether similar interactions between auditory thalamus and auditory cortex in humans will be observable also during auditory fear conditioning remains to be investigated. It is worth to underline the use of fearful faces as CS. This might have specifically elicited the higher evoked power in fusiform gyrus and the higher efferent connectivity from thalamus during CS+ than during CS−. Connectivity between right amygdala and fusiform gyrus discriminates between seen and unseen fear-conditioned faces [Morris et al., 1999] which points to the involvement of fusiform gyrus when faces are used as CS. So, in addition to facilitated sensory processing of CS+ at the relevant cortex [Keil et al., 2007], our findings indicate that fusiform gyrus seem to be part of the fear-conditioning network when faces are used as CS.

In the present study, white noise was used to elicit startle responses and validate in this indirect way the conditioning process. Indeed the startle responses differed significantly only during the conditioning phase. It is probable that the measurement for example of the skin conductivity or the heart rate during the whole experiment would have given a more direct insight to the process of extinction. Extinction in humans is very rapid as compared with animals [for a review see Delgado et al., 2006] especially when a 100% reinforcement schedule is chosen [Skinner, 1953]. This could explain the absence of significant effects at least when using a permutation test accounting for multiple comparisons (effects are seen at an uncorrected level on similar sensors; data not shown). This is in line with previous literature [Miskovic and Keil, 2013; Moratti and Keil, 2005; Moratti et al., 2006]. However, the learnt association is indicated by similar startle responses for CS+ during extinction and conditioning ($P = 0.07$), while they both differ significantly from startle responses for CS+ during habituation. As a last comment, the non-constant duration of the CS (4.6–4.8 sec) was an unconventional choice, however, our analysis is focused on the first 4.5 sec and the behavioral results do indicate that we obtained a pattern common in fear conditioning.

ACKNOWLEDGMENT

This work was performed at Center for Mind/Brain Sciences, CIMeC, University of Trento, Italy.

REFERENCES

Alvarez RP, Biggs E, Chen G, Pine DS, Grillon C (2008): Contextual fear conditioning in humans: Cortical-hippocampal and amygdala contributions. J Neurosci 28:6211–6219.

Apergis-Schoute AM, Debiec J, Doyère V, LeDoux JE, Schafe GE (2005): Auditory fear conditioning and long-term potentiation in the lateral amygdala require ERK/MAP kinase signaling in the auditory thalamus: A role for presynaptic plasticity in the fear system. J Neurosci 25:5730–5739.

Balderston NL, Schultz DH, Baillet S, Helmstetter FJ (2013): How to detect amygdala activity with magnetoencephalography using source imaging. J Vis Exp 76:1–10.

Bardouille T, Ross B (2008): MEG imaging of sensorimotor areas using inter-trial coherence in vibrotactile steady-state responses. NeuroImage 42:323–331.

Bish JP, Martin T, Houck J, Ilmoniemi RJ, Tesche C (2004): Phase shift detection in thalamocortical oscillations using magnetoencephalography in humans. Neurosci Lett 362:48–52.

Brookes MJ, Woolrich M, Luckhoo H, Price D, Hale JR, Stephenson MC, Barnes GR, Smith SM, Morris PG (2011): Investigating the electrophysiology basis of resting state networks using magnetoencephalography. Proc Nat Acad Sci USA 108:16783–16788.

Büchel C, Dolan RJ (2000): Classical fear conditioning in functional neuroimaging early studies using PET. Curr Opin Neurobiol 10:219–223.

Campeau S, Davis M (1995): Involvement of subcortical and cortical afferents to the lateral nucleus of the amygdala in fear conditioning measured with fear potentiated startle in rats trained concurrently with auditory and visual conditioned stimuli. J Neurosci 15:2312–2327.

Clarke S, Riahi-arya S, Tardif E, Eskenasy AC, Probst A (1999): Short communication: Thalamic projections of the fusiform gyrus in man. J Neurosci 11:1835–1838.

Cornwell BR, Frederick WC, Coppola R, Johnson L, Alvarez R Grillon C (2008): Evoked amygdala responses to negative faces revealed by adaptive MEG beamformers. Brain Res 1244:103–112.

Cox RW (1996): AFNI: Software for analysis and visualization of functional magnetic resonance neuroimages. Comput Biomed Res 29:162–173.

Cox RW, Hyde JS (1997): Software tools for analysis and visualization of fMRI data. NMR Biomed 10:171–178.

Das P, Kemp AH, Liddell BJ, Brown KJ, Olivieri G, Peduto A, Williams LM (2005): Pathways for fear perception: Modulation of amygdala activity by thalamo-cortical systems. NeuroImage 26:141–148.

Delgado MR, Olsson E, Phelps EA (2006): Extending animal models of fear conditioning to humans. Biol Psychiatry 73:39–48.

Garcia KS, Steele PM, Mauk MD (1999): Cerebellar cortex lesions prevent acquisition of conditioned eyelid responses. J Neurosci 19:10940–10947.

Guillery R, Sherman S (2002): Thalamic relay functions and their role in corticocortical communication: Generalizations from the visual system. Neuron 33:163–175.

Hansel C, Linden DJ, D'Angelo E (2001): Beyond parallel fiber LTD: the diversity of synaptic and non-synaptic plasticity in the cerebellum. Nat Neurosci 4:467–475.

Hillebrand A, Barnes GR (2002): A quantitative assesssment of the sensitivity of whole-head MEG to activity in the adult human cortex. NeuroImage 638–650.

Jerbi K, Lachaux JP, N'Diaye K, Pantazis D, Leahy RM, Garnero L, Baillet S (2007): Coherent neural representation of hand speed in humans revealed by MEG imaging. Proc Natl Acad Sci USA 104:7676–7681.

Keil A, Stolarova M, Moratti S, Ray WJ (2007): Adaptation in human visual cortex as a mechanism for rapid discrimination of aversive stimuli. NeuroImage 36:472–479.

Knight DC, Cheng DT, Smith CN, Stein EA, Helmstetter FJ (2004): Neural sustrates mediating human delay and trace fear conditioning. J Neurosci 24:218–228.

LaBar KS, Gatenby JC, Gore JC, LeDoux JE, Phelps EA (1998): Human amygdala activation during conditioned fear acquisition and extinction: A mixed-trial fMRI study. Neuron 20:937–945.

Lang PJ, Bradley MM, Cuthbert BN (1990): Emotion, attention and the startle reflex. Physiol Rev 97:377–395.

Langner O, Dotsch R, Bijlstra G, Wigboldus DHLW, Hawk ST van Knippenberg A (2010): Presentation and validation of the Radboud Faces Database. Cogn Emot 24:1377–1388.

Langner R, Kellermann T, Boers F, Sturm W, Willmes K, Eickhoff SB (2011): Modality-specific perceptual expactations selectively modulate baseline activity in auditory, somatosensory and visual cortices. Cereb Cortex 21:2850–2862.

Larson-Prior LJ, Oostenveld R, Della Penna S, Michalareas G, Prior F, Babajani-Feremi A, Snyder AZ, Minn HCPConsortium WU (2013): Adding dynamics to the Human Connectome Project with MEG. NeuroImage 80:190–201.

Ledoux JE, Cicchetti P, Xagoraris A, Romanski LM (1990): The lateral amygdaloid nucleus: Sensory interface of the amygdala in fear conditioning. J Neurosci 10:1062–1069.

LeDoux J (2003): The emotional brain, fear, and the amygdala. Cell Mol Neurobiol 23:727–738.

Lou HC, Gross J, Biermann-Ruben K, Kjaer TW, Schnitzler A (2010): Coherence in consciousness: paralimbic gamma synchrony of self-reference links conscious experiences. Hum Brain Mapp 31:185–192.

Maren S (2001): Neurobiology of Pavlovian fear conditioning. Annu Rev Neurosci 24:897–931.

Maris E, Oostenveld R (2007): Nonparametric statistical testing of EEG and MEG data. J Neurosci Methods 164:177–190.

Martin T, Houck JM, Bish JP, Kicic D, Woodruff CC, Moses SN, Lee DC, Tesche CD (2005): MEG reveals different contributions of somatosensory cortex and cerebellum to simple reaction time after temporally structured cues. Hum Brain Mapp 27: 552–561.

Maschke M, Drepper J, Kindsvater K, Kolb FP, Diener HC, Timmann D (2000): Fear conditioned potentiation of the acoustic blink reflex in patients with cerebellar lesions. J Neurol Neurosurg Psychiatry 68:358–364.

McCarthy G, Puce A, Gore JC, Allison T (1997): Face-specific processing in the human fusiform gyrus. J Cogn Neurosci 9:605–610.

Medendorp WP, Kramer GFI, Jensen O, Oostenveld R, Schoffelen JM, Fries P (2007): Oscillatory activity in human parietal and occipital cortex shows hemispheric lateralization and memory effects in delayed double-step saccade task. Cereb Cortex 17: 2364–2374.

Medina JF, Repa JC, Mauk MD, LeDoux JE (2002): Parallels between cerebellum- and amygdala-dependent conditioning. Nat Rev Neurosci 3:122–131.

Miskovic V, Keil A (2012): Acquired fears reflected in cortical sensory processing: A review of electrophysiological studies of human classical conditioning. Psychophysiology 49:1230–1241.

Miskovic V, Keil A (2013): Perceiving threat in the face of safety: Excitation and inhibition of conditioned fear in human visual cortex. J Neurosci 33:72–78.

Moratti S, Keil A (2005): Cortical activation during Pavlovian fear conditioning depends on heart rate response patterns: An MEG study. Cog Brain Res 25:459–471.

Moratti S, Keil A (2009): Not what you expect: experience but not expectancy predicts conditioned responses in human visual and supplementary cortex. Cereb Cortex 19:2803–2809.

Moratti S, Keil A, Miller GA (2006): Fear but not awareness predicts enhanced sensory processing in fear conditioning. Psychophysiology 43:216–226.

Morris J, Öhman A, Dolan R (1999): A subcortical pathway to the right amygdala mediating "unseen" fear. Proc Natl Acad Sci USA 96:1680–1685.

Nolte G (2003): The magnetic lead field theorem in the quasi-static approximation and its use for magnetoencephalography forward calculation in realistic volume conductors. Phys Med Biol 48:3637–3652.

Nolte G, Ziehe A, Nikulin V, Schlögl A, Krämer N, Brismar T, Müller K-R (2008): Robustly Estimating the Flow Direction of Information in Complex Physical Systems. Phys Rev Lett.

Nolte G, Müller K-R (2010): Localizing and estimating causal relations of interacting brain rhythms. Front Hum Neurosci 4: 209.

Oostenveld R, Fries P, Maris E, Schoffelen JM (2011): FieldTrip: Open source spftware for advanced analysis of MEG, EEG and invasive electrophysiological data. Comp Intell Neurosci ID 156869.

Pastor MA, Artieda J, Arbizu J, Marti-climent JM, Pen I, Masdeu JC (2002): Activation of human cerebral and cerebellar cortex by auditory stimulation at 40 Hz. J Neurosci 22: 10501–10506.

Pessoa L, Adolphs R (2010): Emotion processing and the amygdala: From a 'low road' to 'many roads' of evaluating biological significance. Nat Rev Neurosci 11:773–783.

Phelps EA, Anderson AK (1997): Emotional memory: What does the amygdala do? Curr Biol 7:R311–R314.

Piech RM, McHugo M, Smith SD, Dukic MS, Van Der Meer J, Abou-Khalil B, Zald DH (2010): Fear-enhanced visual search persists after amygdala lesions. Neurophysiologia 48:3430–3435.

Poch C, Fuentemilla L, Barnes GR, Düzel E (2011): Hippocampal theta-phase modulation of replay correlates with configural-relational short-term memory performance. J Neurosci 31: 7038–7042.

Quaraan MA, Moses SAN, Hung Y, Mills T, Taylor MJ (2010): Detection and localization of hippocampal activity using beamformers with MEG: A detailed investigation using simulations and empirical data. Hum Brain Mapp 32:812–827.

Quirk GJ, Armony JL, Ledoux JE (1997): Components of tone-evoked spike trains in auditory cortex and lateral amygdala. Neuron 19:613–624.

Rao SM, Mayer AR, Harrington DL (2001): The evolution of brain activation. Nat Neurosci 4:317–323.

Rescorla RA (1968): Probability of shock in the presence and absence of CS in fear conditioning. J Comp Physiol Psychol 66: 1–5.

Romanski LM, LeDoux JE (1992): Equipotentiality of thalamo-amygdala and thalamo-corticoamygdala circuits in auditory fear conditioning. J Neurosci 12:4501–4509.

Roux F, Wibral M, Singer W, Aru J, Uhlhaas PJ (2013): The phase of thalamic alpha activity modulates cortical gamma-band activity: Evidence from resting-state MEG recordings. J Neurosci 33:17827–17835.

Sacchetti B, Baldi E, Lorenzini CA, Bucherelli C (2002): Cerebellar role in fear-conditioning consolidation. Proc Natl Acad Sci USA 99:8406–8411.

Sehlmeyer C, Schöning S, Zwitserlood P, Pfleiderer B, Kircher T, Arolt V, Konrad C (2009): Human fear conditioning and extinction in neuroimaging: A systematic review. PLoS One 4: e5865

Shi C, Davis M (2001): Visual pathways involved in fear conditioning measured with fear-potentiated startle: Behavioral and anatomic studies. J Neurosci 21:9844–9855.

Shipp S (2003): The functional logic of cortico-pulvinar connections. Phil Trans R Soc Lond B 358:1605–1624.

Shipp S (2004): The brain circuitry of attention. Trends Cogn Sci 2: 223–230.

Skinner (1953): The Possibility of a Science of Human Behavior. New York: The Free Press.

Spencer RMC, Zelaznik HN, Diedrichsen J, Ivry RB (2003): Disrupted timing of discontinuous but not continuous movements by cerebellar lesions. Science 300:1437–1439.

Stolarova M, Keil A, Moratti S (2006): Modulation of the C1 visual event-related component by conditioned stimuli: Evidence for sensory plasticity in early affective perception. Cereb Cortex 16:876–887.

Sun FT, Miller LM, D'Esposito M (2004): Measuring interregional functional connectivity using coherence and partial coherence analyses of fMRI data. NeuroImage 21:647–658.

Tarkiainen A, Liljestrom M, Seppa M, Salmelin R (2003): The 3D topography of MEG source localization accuracy: Effects of conductor model and noise. Clin Neurophysiol 114:1977–1992.

Tesche CD, Karhu J (2000a): Theta oscillations index human hippocampal activation during a working memory task. Proc Natl Acad Sci USA 97:919–924.

Tesche CD, Karhu J (2000b): Anticipatory cerebellar responses during somatosensory omission in man. Hum Brain Mapp 9: 119–142.

Timmermann L, Gross J, Dirks L, Volkman J, Freund HJ, Schnitzler A (2002): The cerebellar oscillatory network of Parkinsonian resting tremor. Brain 126:199–212.

Tsuchiya N, Moradi F, Felsen C, Yamazaki M, Adolphs R (2009): Intact rapid detection of fearful faces in the absence of the amygdala. Nat Neurosci 12:1224–1225.

van Veen BD, van Drongelen W, Yuchtman M, Suzuki A (1997): Localization of brain electrical activity via linearly constrained minimum variance spatial filtering. IEEE Trans Biomed Eng 44:867–880.

Victor JD, Mast J (1991): A new statistic for steady-state evoked potentials. Electroencephalo Clin Neurophysiol 78:378–388.

Vuilleumier P, Armony JL, Driver J, Dolan R (2001): Effects of attention and emotion on face processing in the human brain: An event-related fMRI study. Neuron 30:829–841.

Vuilleumier P (2005): How brains beware: neural mechanisms of emotional attention. Trends Cogn Sci 9:585–594.

Vuilleumier P, Driver J (2007): Modulation of visual processing by attention and emotion: Windows on causal interactions between human brain regions. Philos Trans R Soc Lond Biol Sci 362:837–855.

Weinberger NM (2011): The medial geniculate, not the amygdala, as the root of auditory fear conditioning. Hearing Res 274:61–74.

Weisz N, Lecaignard F, Müller N, Bertrand O (2012): The modulatory influence of a predictive cue on auditory steady-state response. Hum Brain Mapp 33:1417–1430.

White EL (1979): Thalamocortical synaptic relations: A review with emphasis on the projections of specific thalamic nuclei to the primary sensory areas of the neocortex. Brain Res Rev 1:275–311.